Insulin restores UCP3 activity and decreases energy surfeit to alleviate lipotoxicity in skeletal muscle

WENJUAN TANG, SUNYINYAN TANG, HONGDONG WANG, ZHIJUAN GE, DALONG ZHU and YAN BI

Department of Endocrinology, Drum Tower Hospital Affiliated to Nanjing University Medical School, Nanjing, Jiangsu 210008, P.R. China

Received March 12, 2017; Accepted September 19, 2017

DOI: 10.3892/ijmm.2017.3169

Abstract. An early insulin regimen ameliorates glucotoxicity but also lipotoxicity in type 2 diabetes; however, the underlying mechanism remains elusive. In the present study, we investigated the role of mitochondria in lipid regulation following early insulin administration in insulin-resistant skeletal muscle cells. Male C57BL/6 mice, fed a high-fat diet (HFD) for 8 weeks, were treated with insulin for 3 weeks, and L6 myotubes cultured with palmitate (PA) for 24 h were incubated with insulin for another 12 h. The results showed that insulin facilitated systemic glucose disposal and attenuated muscular triglyceride accumulation *in vivo*. Recovery of AMP-activated protein kinase (AMPK) phosphorylation, inhibition of sterol-regulated element binding protein-1c (SREBP-1c) and increased carnitine palmitoyltransferase-1B (CPT1B) expression were observed after insulin administration. Moreover, increased ATP concentration and cellular energy charge elicited by over-nutrition were suppressed by insulin. Despite maintaining respiratory complex activities, insulin restored muscular uncoupling protein 3 (UCP3) protein expression *in vitro* and *in vivo*. By contrast, knockdown of UCP3 abrogated insulin-induced restoration of AMPK phosphorylation *in vitro*. Importantly, the PA-induced decrease in UCP3 was blocked by the proteasome inhibitor MG132, and insulin reduced UCP3 ubiquitination, thereby prohibiting its degradation. Our findings, focusing on energy balance, provide a mechanistic understanding of the promising effect of early insulin initiation on lipotoxicity. Insulin, by recovering UCP3 activity, alleviated energy surfeit and potentiated AMPK-mediated lipid homeostasis in skeletal muscle cells following exposure to PA and in gastrocnemius of mice fed HFD.

Correspondence to: Professor Yan Bi or Professor Dalong Zhu, Department of Endocrinology, Drum Tower Hospital Affiliated to Nanjing University Medical School, 321 Zhongshan Road, Nanjing, Jiangsu 210008, P.R. China
E-mail: biyan@nju.edu.cn
E-mail: zhudalong@nju.edu.cn

Abbreviations: AMPK, AMP-activated protein kinase; CPT1B, carnitine palmitoyltransferase 1B; FBG, fasting blood glucose; HFD, high-fat diet; HOMA-IR, homeostasis model assessment of the insulin resistance index; MG132, carbobenzoxy-Leu-Leu-leucinal; NPH, neutral protamine Hagedorn; PA, palmitate; SREBP-1c, sterol-regulated element binding protein-1c; T2DM, type 2 diabetes mellitus; UCP3, uncoupling protein 3; VDAC1, voltage-dependent anion-selective channel 1, ATP, adenosine triphosphate; ADP, adenosine diphosphate; AMP, adenosine monophosphate

Key words: early insulin administration, energy charge, muscular lipotoxicity, uncoupling protein 3

Introduction

In tandem with the global obesity pandemic, type 2 diabetes mellitus (T2DM) has become a major public health issue (1). In traditional glycemic management based on a stepwise approach, insulin is considered as only the final alternative. Nevertheless, emerging evidence indicates that early initiation of insulin extended glycemic remission, by preserving β-cell function, in newly onset T2DM (2). Moreover, systemic insulin sensitivity was also improved after early insulin administration (3,4). The underlying mechanism, however, remains obscure.

Lipotoxicity describes the deleterious effects of ectopic fat deposition on glucose metabolism in insulin-responsive tissues, playing a pivotal role in the pathogenesis of obesity-associated insulin resistance (5). Insulin-mediated myocellular glucose uptake is capital in maintaining systemic glucose homeostasis (6). Along with the intramuscular lipid accumulation, enriched lipid intermediates impede the insulin signaling cascade and stimulate inflammation and endoplasmic reticulum stress, causing muscular insulin resistance (7-9). Triglyceride content relies on the equilibrium between *de novo* lipogenesis and fatty acid oxidation. Sterol-regulated element binding protein-1c (SREBP-1c) is a master regulator of lipogenesis, controlling the transcription and expression of lipogenic enzymes. It is well-established that the physiological SREBP-1c expression is increased by insulin and nutrition availability (10-12). On the other hand, β-oxidation is modulated by carnitine palmitoyltransferase 1B (CPT1B), the rate-limiting enzyme mainly expressed in skeletal muscle, to transport fatty acids into mitochondria for oxidation. Individuals with insulin resistance have reduced capacity of fatty acid oxidation in skeletal muscle, resulting from suppressed CPT1B activity (13-15). Both SREBP-1c and CPT1B are regulated by AMP-activated protein kinase (AMPK), which responds to various nutritional

cues in order to balance the production of ATP corresponding to the demand (16,17). Once activated, the phosphorylated AMPK induces CPT1B to switch-on catabolism and inhibits SREBP-1c to restrain anabolism. Different from the sustained AMPK activity in the vastus lateralis of T2DM patients during a euglycemic-hyperinsulinemic clamp (18), we previously uncovered that continuous subcutaneous insulin intervention improved AMPK phosphorylation in the gastrocnemius of diabetic mice (19).

The occurrence of obesity-associated insulin resistance can be traced to a chronic state of energy surfeit (20), which is detrimental to AMPK activation. The adenylate energy charge, calculated as [ATP + 0.5 x ADP]/[ATP + ADP + AMP], is an integrated index of cellular energy status. This value is increased with excessive calorie intake or a sedentary lifestyle, while energy deficiency caused by hunger and exercise abates it. Lipid biosynthesis is promoted to store energy when increased delivery of calories overwhelms the expenditure (5). Thus, uncoupling protein 3 (UCP3) is a focus of intensive research for protecting against lipid deposition in skeletal muscle, owing to its inhibitory effect on ATP production (20,21). UCP3-mediated proton-leak across the mitochondrial inner membrane eliminates the driving force of ATP synthesis, and then creates a futile cycle of substrate oxidation. Clinical observations have found that both mRNA and protein expression of UCP3 were reduced in skeletal muscle of pre-diabetic and T2DM populations (22-24). Additional experimental evidence supports the protective role of UCP3 in conditions of energy overload. UCP3 transgenic mice are lean and resistant to high-fat diet (HFD)-induced obesity, which is attributable to decreased metabolic efficiency (25-27). Although accumulating evidence indicates that instant insulin-stimulated muscular ATP synthesis is abolished in T2DM patients (28,29), the impact of an early insulin regimen on energy metabolism or UCP3 expression in skeletal muscle with insulin resistance and its correlation to lipid amelioration remain poorly understood.

Here, we investigated the effect of insulin on muscular lipid metabolism and the underlying mechanisms in the early phase of insulin resistance *in vivo* and *in vitro*, with a focus on the regulation of energy balance. We found that by recovering UCP3 activity, insulin blocked ATP surplus and restored AMPK phosphorylation to alleviate lipid accumulation in skeletal muscle cells exposed to palmitate (PA) and in gastrocnemius in mice fed HFD. Our data provide insight into the promising effects of insulin on lipid metabolism and insulin sensitivity in the early course of diabetes.

Materials and methods

Reagents and antibodies. PA, insulin and carbobenzoxy-Leu-Leu-leucinal (MG132) were obtained from Sigma-Aldrich (St. Louis, MO, USA). Antibodies against voltage-dependent anion-selective channel 1 (rabbit polyclonal to VDAC1, ab34726, 1:5,000), NADH dehydrogenase [ubiquinone] 1α subcomplex subunit 9 (rabbit monoclonal to NDUFA9, ab181381, 1:1,000), ubiquinol cytochrome *c* reductase core protein 2 (mouse monoclonal to UQCRC2, ab14745, 1:1,000), ATP synthase subunit α (mouse monoclonal to ATP5A, ab110273, 1:4,000) and UCP3 (rabbit polyclonal, ab3477, 1:2,000) were purchased from Abcam (Cambridge, MA, USA). Anti-IgG (normal goat IgG, sc-2028, 1:1,000), anti-ubiquitin (rabbit polyclonal, sc-9133, 1:1,000), anti-UCP3 for immunoprecipitation (goat polyclonal, sc-31387, 1:2,000) and anti-SREBP-1c antibodies (rabbit monoclonal, sc-8984, 1:5,000) were acquired from Santa Cruz Biotechnology, Inc. (Santa Cruz, CA, USA). Antibodies against succinate dehydrogenase complex subunit A (rabbit monoclonal to SDHA, 11998, 1:2,000), cytochrome *c* oxidase subunit IV (rabbit monoclonal to COX IV, 4850, 1:500), AMPKα (rabbit monoclonal, 2603, 1:2,000) and p-AMPKα (Thr172) (rabbit monoclonal, 2535, 1:1,000) were obtained from Cell Signaling Technology (Danvers, MA, USA). The anti-CPT1B antibody was obtained from Absin Bioscience Inc. (Beijing, China) (rabbit polyclonal, abs117445, 1:5,000).

Animal experiments. Male C57BL/6J mice were obtained from the Comparative Medicine Centre of Yangzhou University (Yangzhou, China) at 6 weeks of age. All mice were maintained under standard light (12 h light/dark), temperature (22±2˚C), and humidity (40±10%) conditions with *ad libitum* access to food and water. Mice were randomized into an HFD group (D12492, 60% calories from fat, 21% calories from carbohydrates, and 19% calories from protein; obtained from Guangdong Medical Laboratory Animal Center, Guangzhou, China) at 8 weeks to establish a diet-induced obese (DIO) model. The control mice were fed with chow diet (10% calories from fat, 70% calories from carbohydrates and 20% calories from protein). After an 8-week feeding, weight- and glucose-matched DIO mice were further assigned randomly into a neutral protamine Hagedorn (NPH) insulin (0.4-0.6 U/day, subcutaneous; Novo Nordisk A/S, Maaloev, Denmark) or a saline treatment group for a total of 3 weeks, during which all animals continued on their original diets (n=8/group). The NPH insulin was titrated to a glycemic target of nonfasting blood glucose level <8 mmol/l in a week. Individual body weight and fasting glucose concentration were monitored every week. Three weeks later, mice were fasted for 14 h and challenged with an intraperitoneal glucose tolerance test (IPGTT, intraperitoneal D-glucose load, 2 g/kg body weight). Glucose levels were assessed in duplicate by glucometer with tail vein blood samples at 0, 30, 60 and 120 min after glucose administration. After being deprived of food for 10 h without insulin intervention overnight, mice were sacrificed for fasting blood and tissue collection. Gastrocnemius was dissected from any visible adipose tissue and stored at -80˚C for further analysis. All of the animal procedures were performed according to the National Institutes of Health Guidelines and approved by the Animal Care Committee of Drum Tower Hospital, which is affiliated with Nanjing University Medical School, Nanjing, China.

Biochemical assay. Fasting serum insulin and triglyceride contents, and prepared gastrocnemius triglyceride samples (30) were analyzed with ELISA kits (CEA448Mu and CEB687Ge; Cloud-Clone Corp., Houston, TX, USA) accordingly.

Cell culture. L6 myoblasts were obtained from the Chinese Academy of Sciences (Shanghai, China). They were cultured in Dulbecco's modified Eagle's medium (DMEM) supplemented

with 10% fetal bovine serum (FBS) (vol/vol), and differentiated into myotubes with medium containing 2% FBS (vol/vol), as previously described (31). L6 myotubes pre-incubated in serum-free medium for 8 h were treated with 500 μmol/l PA for 24 h, and then another 12 h with 100 nmol/l insulin. Where indicated, differentiated L6 myotubes were pretreated with MG132 (5 μmol/l) for 48 h prior to PA (32). The appropriate vehicle served as the control.

siRNA transfection. L6 myoblasts were transfected with siRNA oligonucleotides (20 nmol/l, AM16708) using Lipofectamine RNAiMAX (13778150) (both from Invitrogen, Grand Island, NY, USA). Cells were cultured for 36 h prior to PA and insulin addition. The sequence of the stealth RNAi against *ucp3* is as follows: 5'-GGGACUUGGCCCAACAUCACAAGAA-3'. Stealth RNAi negative control with low GC content (12935111; Invitrogen) was used as control.

Quantitative (real-time) PCR. The mtDNA copy number was evaluated from genomic DNA prepared using the DNeasy Blood and Tissue kit (69504; Qiagen, Hilden, Germany). Real-time PCR was used to quantify amplifications of mtDNA with both sense and antisense primers (mtDNA forward, 5'-CCC CAGAGGATTAAACTCCAACGCA-3' and reverse, 5'-GGG TGGGGTCAGGGGGT-3'; 18s RNA forward, 5'-TTGGGA TGGGAAAGATGGG-3' and reverse, 5'-CAGAGTAGGAGG GAACAAGTGT GAC-3'), at a final volume of 20 μl using the QuantiNova SYBR-Green PCR kit (Qiagen) with an ABI StepOne Real-Time PCR system (Applied Biosystems, Grand Island, NY, USA). The thermal cycling conditions were as follows: 2 min at 95˚C, and then 40 cycles of 5 sec at 95˚C, 10 sec at 60˚C. Dissociation curves were plotted to ensure primer specificity. The $\Delta\Delta$Ct method was applied for calculation (33).

Western blot analysis. L6 myotubes and gastrocnemius fragments were washed twice with cold phosphate-buffered saline and lysed in RIPA lysis buffer with Protease Inhibitor Cocktail (Roche, Basel, Switzerland). Total protein concentrations were determined using the bicinchoninic acid (BCA) method. Twenty micrograms of protein per sample were separated on sodium dodecyl sulfate-polyacrylamide gel electrophoresis (SDS-PAGE) gel and then transferred to polyvinylidene difluoride membranes, which were blocked with 5% nonfat milk (wt/vol) in Tris-buffered saline with 0.1% Tween-20 (TBST) and incubated with corresponding primary antibodies overnight at 4˚C. The membranes were washed with TBST and incubated with an appropriate secondary antibody (goat anti-mouse IgG, GAM0072, and rabbit anti-goat IgG, RAG0072; both from MultiSciences Biotech, Suzhou, China; and goat anti-rabbit IgG, ZB-2301; ZSGB-BIO, Beijing, China) at room temperature for ~2 h. The signals were visualized by enhanced chemiluminescence (EMD Millipore, Billerica, MA, USA) and quantified by densitometry (Quantity One; Bio-Rad, Hercules, CA, USA).

ATP assay. AMP, ADP and ATP contents from cell samples were measured with high performance liquid chromatography. Briefly, the frozen cells were lysed in 500 μl ice-cold 0.6 mol/l perchloric acid and centrifuged at 13,000 x g for 2 min at 4˚C. The supernatant was neutralized by 1 ml ice-cold freon/trioctylamine (4:1 vol/vol). Then the upper aqueous layer was collected after centrifugation (13,000 x g for 2 min at 4˚C) for chromatographic separation and analysis (34). As to skeletal muscle tissues, ATP was measured with the ATP assay kit (S0027; Beyotime Institute of Biotechnology, Shanghai, China) immediately after tissue isolation. The supernatants were collected following homogenate and centrifugation (12,000 x g for 5 min at 4˚C), and then added to the reaction mixture. The luminescent signals were detected by the luminometer (GloMax; Promega Corp., Madison, WI, USA). The ATP concentrations were normalized to the protein concentration.

Isolation of mitochondria and detection of mitochondrial membrane potential. L6 myotubes and gastrocnemius fragments were suspended with ice-cold isolation agent containing PMSF (C3601; Beyotime Institute of Biotechnology). The samples were then homogenized gently and centrifuged twice at 4˚C (1,000 x g for 10 min and then 3,500 x g for 10 min). Mitochondria were collected as a pellet and resuspended for functional analysis.

Mitochondrial membrane potential was assessed by JC-1 staining (GMS10013; Genmed Scientifics Inc., Wilmington, DE, USA) immediately after mitochondrial isolation. Purified mitochondria were mixed with the JC-1 reagent, and the relative fluorescence unit (RFU) was detected at λ ex/em 490/590 nm on a fluorescence microplate reader (SpectraMax M3; Molecular Devices, Sunnyvale, CA, USA).

Respiratory complex activities. The activities of mitochondrial complexes in L6 myotubes were evaluated by a colorimetric method according to the protocol of the manufacturer (Genmed Scientifics Inc.).

Co-immunoprecipitation. Skeletal muscle tissues were lysed with NP-40 lysis buffer containing PMSF and cocktail. After homogenization and centrifugation (12,000 x g for 15 min at 4˚C), the supernatants were pre-cleared with 10 μl protein A/G Plus agarose beads (sc-2003; Santa Cruz Biotechnology, Inc.) for 2 h. Then the lysates were incubated with anti-UCP3 antibody (2 μg/100-500 μg of total protein) overnight, followed by co-incubating with 20 μl protein A/G Plus agarose beads for another 5 h. The beads were washed three times with NP-40 lysis buffer with PMSF and cocktail. All the procedures above were manipulated at 4˚C. The precipitated proteins were separated from beads by heating in boiling water for 10 min, and analyzed by western blot analysis.

Statistical analysis. Data are presented as means ± SEM. Differences between multiple groups were analyzed by one-way ANOVA with the least significant difference (LSD) or Dunnett's T3 post hoc comparison analysis as appropriate. A P-value <0.05 was considered to indicate a statistically significant difference.

Results

Early insulin therapy attenuates triglyceride deposition in skeletal muscle in vivo. Compared with the HFD-fed mice, insulin treatment for 3 weeks markedly decreased the

Table I. Characteristics of the experimental animals at the end of the intervention study.

	NC	HFD	INS
Body weight (g)	26.17±0.67	33.02±0.84[a]	32.29±0.86
Fasting blood glucose (mmol/l)	5.53±0.52	7.82±0.34[a]	4.82±0.31[b]
Fasting insulin (pg/ml)	1,341.53±52.57	1,177.94±119.4	511.08±85.22[b]
HOMA-IR	1.000±0.13	1.34±0.16	0.48±0.09[b]
AUC for IPGTT (mmol/l x min)	1,520.5±80.73	2,726.4±42.28[a]	2022.5±76.02[b]
Fasting triglyceride (μg/ml)	49.91±3.60	73.41±14.09	35.29±3.23[c]
Muscle triglyceride (μg/ml x mg wet tissue)	4.29±0.33	6.02±0.38[a]	4.83±0.18[c]

NC, normal chow diet; HFD, HFD-fed mice with saline; INS, HFD-fed mice treated with insulin (n=4-8/group); HOMA-IR, homeostasis model assessment of the insulin resistance index; AUC, areas under the curve; IPGTT, intraperitoneal glucose tolerance test. Data are presented as means ± SEM. [a]P<0.01 vs. NC; [b]P<0.01 and [c]P<0.05 vs. HFD.

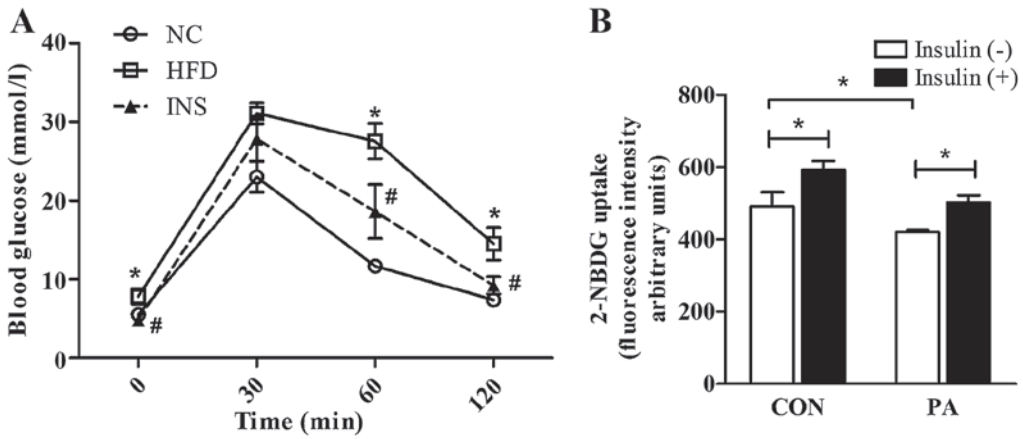

Figure 1. Early insulin administration improves systemic glucose homeostasis in high-fat diet (HFD)-fed mice [(A) n=4-8/group] and glucose uptake in L6 myotubes [(B) n=3/group]. For (A): NC, normal chow diet; HFD, HFD-fed mice with saline; INS, HFD-fed mice treated with insulin. *P<0.05 vs. NC; #P<0.05 vs. HFD. For (B): CON, BSA-induced L6 myotubes; PA, palmitate-induced L6 myotubes. *P<0.05 as indicated. Values are expressed as means ± SEM.

fasting blood glucose (FBG), fasting serum insulin level, and HOMA-IR despite the stabilized body weight (Table I). In addition, the IPGTT showed that systemic glucose clearance was improved by insulin (Fig. 1A). Concomitantly, the glucose areas under the curve (AUC) were decreased after insulin therapy (Table I). *In vitro*, insulin also ameliorated the impaired capacity of glucose uptake in the PA-pretreated L6 myotubes (Fig. 1B).

In contrast to the normal chow (NC) group, HFD mice demonstrated a prominent triglyceride accumulation in the gastrocnemius, which was notably alleviated by insulin. Moreover, the insulin-treated mice had lower serum triglyceride level than that noted in the HFD-fed mice (Table I).

Insulin restores AMPK phosphorylation to facilitate fatty acid oxidation and suppress lipogenesis. The disturbance between lipogenesis and fatty acid oxidation contributes to lipid deposition. Thus, AMPK (the metabolic modulator), SREBP-1c and CPT1B were examined in skeletal muscle cells. In comparison to NC, HFD-fed mice had reduced muscular AMPK phosphorylation, increased SREBP-1c and similar CPT1B expression. Strikingly, after insulin administration, the expression of CPT1B was upregulated and that of SREBP-1c was suppressed, accompanied by recovered AMPK phosphorylation (Fig. 2A). Likewise, *in vitro*, insulin restored p-AMPK and CPT1B expression, and attenuated SREBP-1c expression in L6 myotubes after exposure to PA (Fig. 2B). These results indicated that AMPK-associated SREBP-1c and CPT1B regulation participated in the interplay of saturated fatty acid and insulin on triglyceride deposition in skeletal muscle.

Insulin alleviates energy surfeit through dissipating mitochondrial membrane potential in skeletal muscle cells exposed to excessive fatty acid. AMPK activation is sensitive to the ratio of AMP:ATP in targeting metabolic processes, thus serving as an energy sensor. To address the effect of saturated fatty acid and insulin on muscular adenylate energy metabolism, AMP, ADP and ATP contents were detected and the adenylate energy charge was calculated. In L6 myotubes, the PA exposure promoted a significant augmentation of ATP content and energy charge, leading to a decline in the AMP:ATP ratio. Insulin was observed to abrogate the increase in ATP and energy charge, thereby raising the AMP:ATP ratio (Fig. 3A). Similarly, insulin alleviated the ATP overload

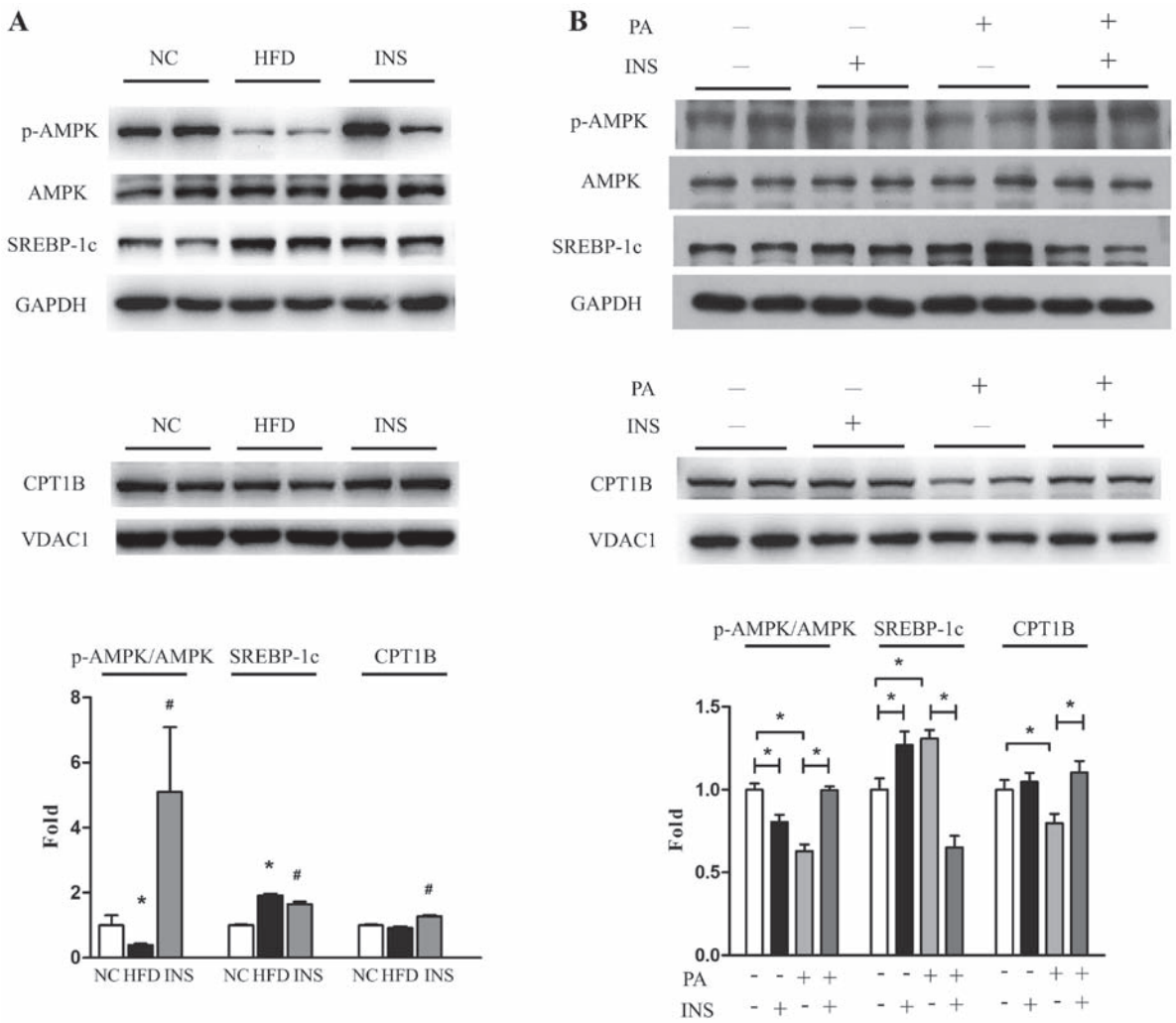

Figure 2. Insulin restores AMP-activated protein kinase (AMPK) signaling in skeletal muscle cells exposed to excessive fatty acid. The muscular protein levels of p-AMPK/AMPK, sterol-regulated element binding protein-1c (SREBP-1c) and carnitine palmitoyltransferase 1B (CPT1B) were determined by western blotting *in vivo* (A) and *in vitro* (B). For (A): NC, normal chow diet; HFD, high-fat diet-fed mice with saline; INS, HFD-fed mice treated with insulin. *P<0.05 vs. NC; #P<0.05 vs. HFD. For (B): PA, palmitate; INS, insulin. *P<0.05 as indicated. Values are presented as mean ± SEM for at least 3 independent experiments.

in the gastrocnemius of HFD-fed mice (Fig. 3B). Moreover, a positive correlation between ATP and muscle triglyceride was observed (r=0.745; P=0.013).

Given that mitochondrial content, mitochondrial membrane potential and ATP synthase are the major determinants of ATP synthesis in the organelle, these were estimated to identify the precise mechanism of ATP regulation. Results showed that neither PA nor insulin exerted any significant effect on mtDNA content in the L6 myotubes (Fig. 3C). Both the protein expression and the activity of ATP synthase were not significantly altered after PA or insulin administration (Fig. 3D and E). However, notably, the muscular level of mitochondrial membrane potential was stimulated in the presence of fatty acid but predominantly declined after insulin intervention *in vivo* and *in vitro* (Fig. 3F and G).

Mitochondrial membrane potential is a proton electrochemical gradient, which is established by respiratory complexes. Therefore, we evaluated the protein expression and activities of all the respiratory complexes in an attempt to ascertain the molecules responsible for mitochondrial membrane potential alteration. PA exerted a neutral impact on the protein levels of mitochondrial complexes, consisting of NDUFA9 (complex I subunit), SDHA (complex II subunit), UQCRC2 (complex III subunit), and COX4 (complex IV subunit). In addition, only the activities of complex III and IV were promoted by PA. Nonetheless, in the presence of PA, neither the expression nor the activities of respiratory complexes were affected by insulin (Fig. 3H and I).

Insulin, by inhibiting degradation, restores the UCP3 protein level which contributes to the preservation of AMPK phosphorylation. Apart from respiratory complexes, mitochondrial membrane potential could also be affected by UCP3 in skeletal muscle. *In vitro*, the UCP3 protein level was attenuated ~40% in the PA-treated L6 myotubes; however, this inhibition was relieved markedly by insulin, thereby dissipating the proton motive force. The restoration of UCP3 protein by insulin was also observed in the gastrocnemius of mice provided with HFD (Fig. 4A).

Considering that the rapid turnover of UCP3 is attributable to the ubiquitin-proteasome system (35,36), MG132, a pharmacological inhibitor of 26S proteasome, was used to pretreat L6 myotubes prior to PA. The results showed that the PA-induced decrease in UCP3 protein expression

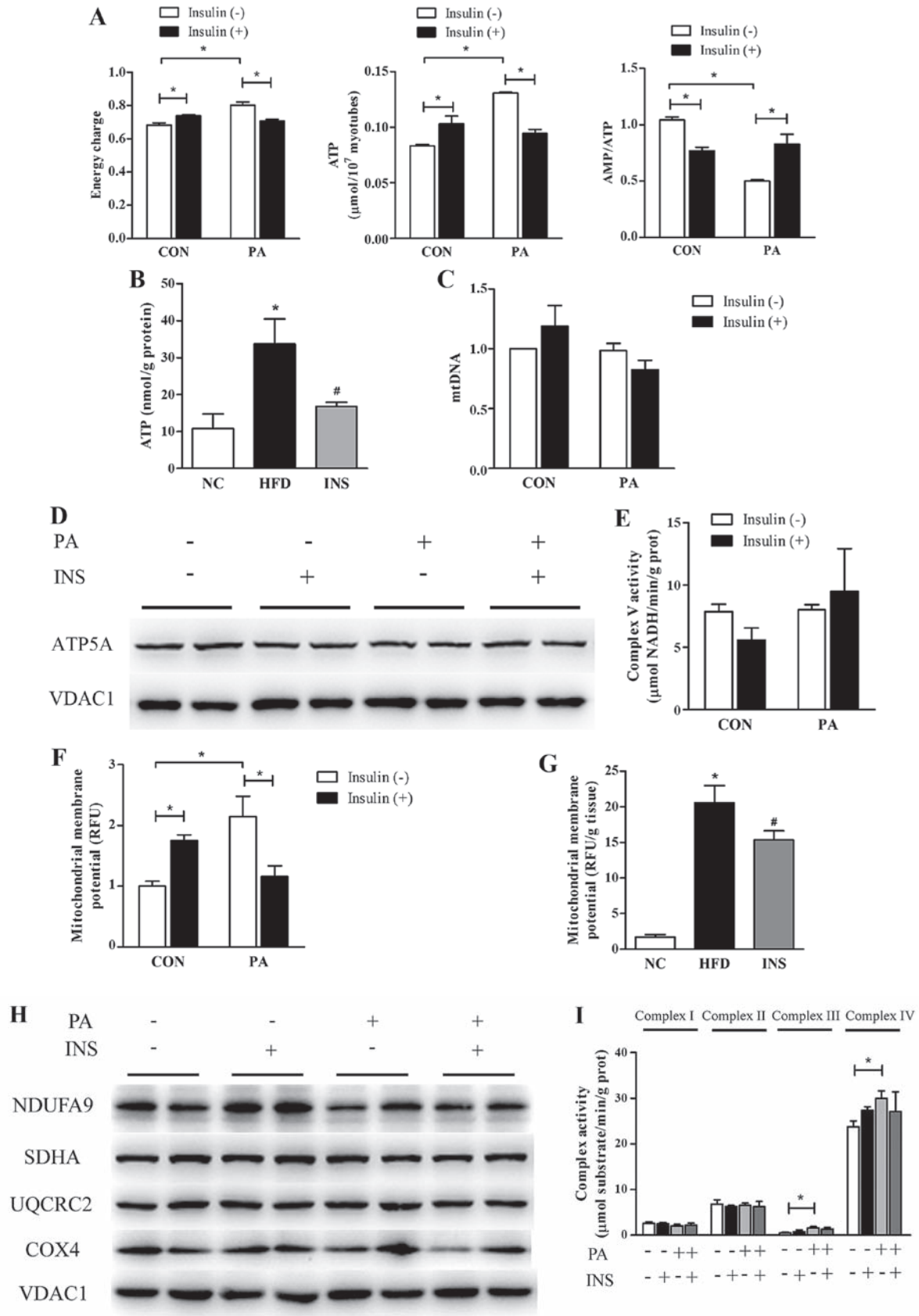

Figure 3. Insulin alleviates the energy surplus and mitochondrial membrane potential stimulation in skeletal muscle cells with a surfeit of fatty acid. (A) The cellular adenylate energy charge level, ATP content, and AMP:ATP ratio were assessed in L6 myotubes with PA and insulin intervention (n=3/group). (B) The ATP content of gastrocnemius was determined in the three groups of mice (n=5-6/group). (C-E) PA and insulin had little effects on mitochondrial quantity (evaluated by mtDNA) or ATP synthase in L6 myotubes (n=4/group). (F and G) Mitochondrial membrane potential levels were evaluated in L6 myotubes (n=3/group) and in gastrocnemius of mice (n=3-6/group). (H and I) The effects of PA and insulin on protein expression and activities of respiratory complexes in L6 myotubes (n=3/group). For (A, C, E and F): CON, BSA-induced L6 myotubes; PA, PA-induced L6 myotubes. *P<0.05 as indicated. For (B and G): NC, normal chow diet; HFD, high-fat diet-fed mice with saline; INS, HFD-fed mice treated with insulin. *P<0.05 vs. NC; $^{\#}$P<0.05 vs. HFD. For (I): PA, palmitate; INS, insulin. *P<0.05 as indicated. Values are expressed as means ± SEM.

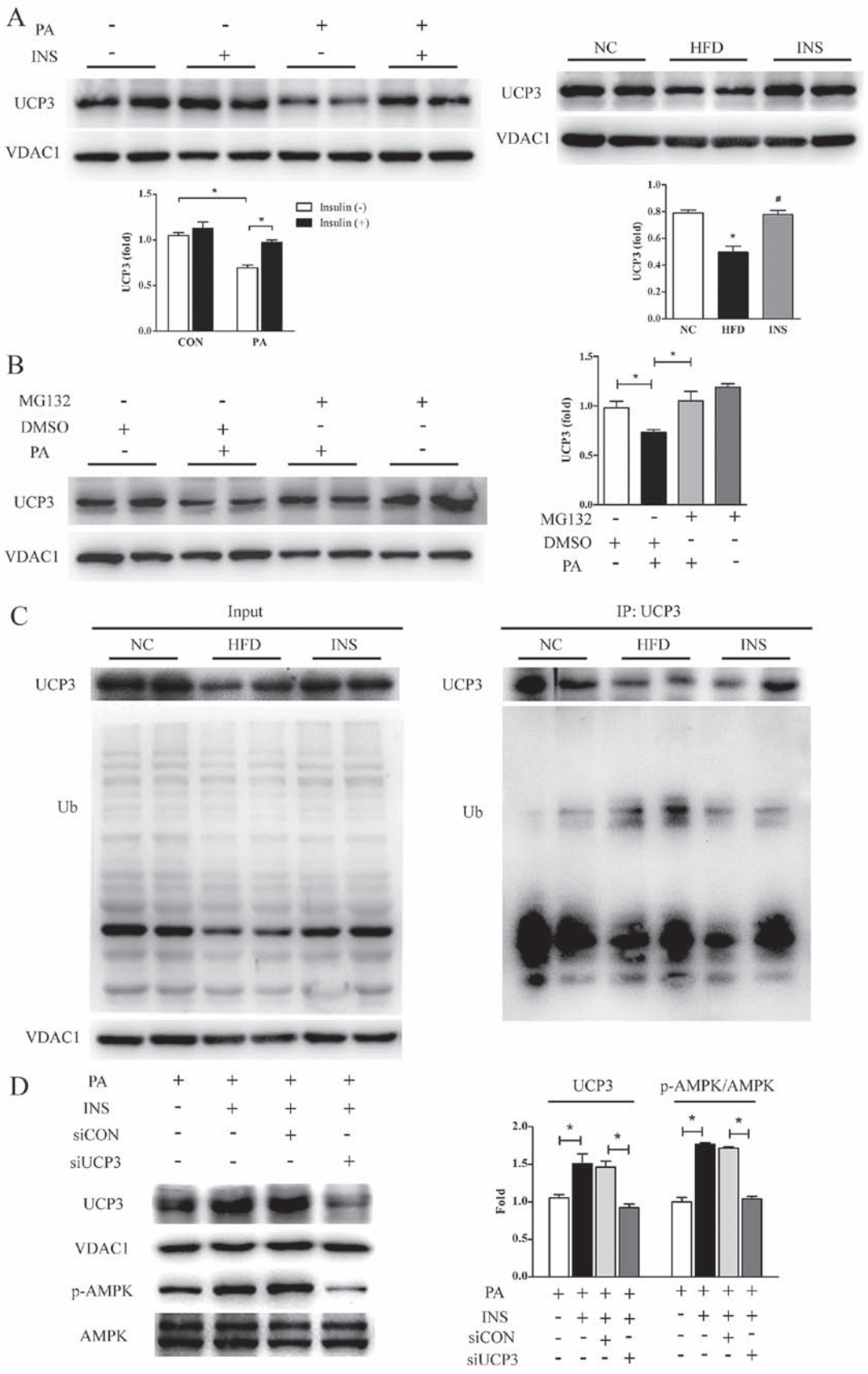

Figure 4. Uncoupling protein 3 (UCP3) protein expression is restored after insulin intervention in skeletal muscle cells provided with excessive fatty acid and mediated insulin-induced augmentation of AMP-activated protein kinase (AMPK) phosphorylation. (A) The UCP3 protein level in response to fatty acid and insulin was determined by western blotting in L6 myotubes and gastrocnemius of mice. CON, BSA-induced L6 myotubes; PA, PA-induced L6 myotubes. *P<0.05 as indicated. (B) The UCP3 protein expression was determined by western blotting in PA-induced L6 myotubes with or without MG132 pretreatment. *P<0.05 as indicated. (C) The effects of high-fat diet (HFD) and insulin on UCP3 ubiquitination in mouse gastrocnemius were assessed by co-immunoprecipitation. (D) The effect of siRNA-UCP3 on p-AMPK/AMPK protein level after insulin treatment was determined in PA-treated myotubes. *P<0.05 as indicated. For (A and C): NC, normal chow diet; HFD, HFD-fed mice with saline; INS, HFD-fed mice treated with insulin. *P<0.05 vs. NC; #P<0.05 vs. HFD. Values are presented as means ± SEM for at least 3 independent experiments.

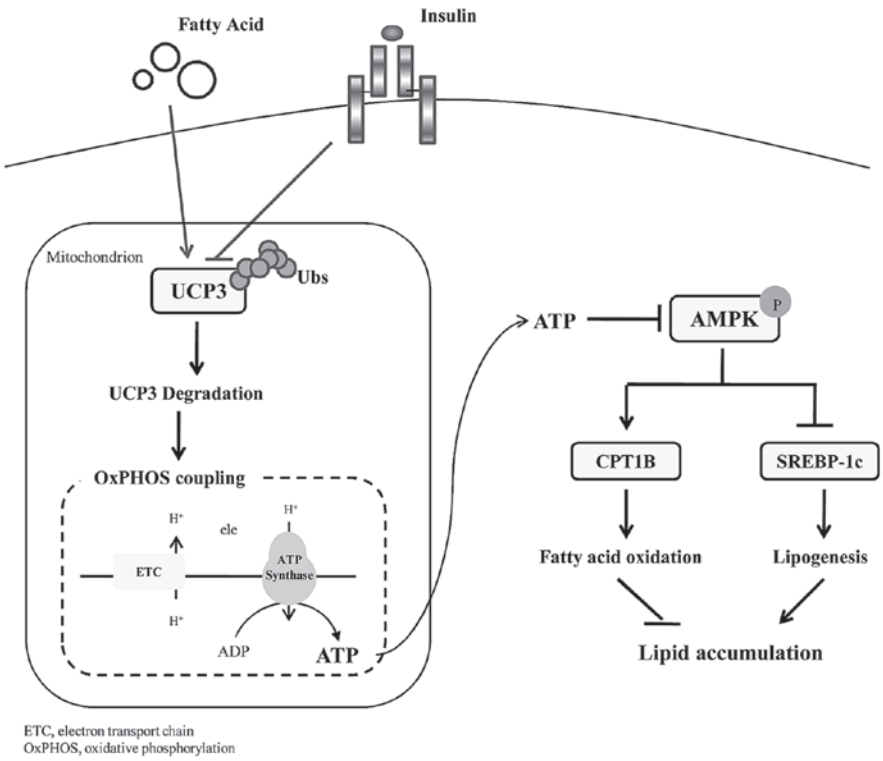

Figure 5. Mechanistic model based on our study. Early insulin administration alleviates muscular energy overload via repressing uncoupling protein 3 (UCP3) ubiquitination and hence restoring its protein expression, which resulted in activation of AMP-activated protein kinase (AMPK) signaling to improve lipid homeostasis.

was annulled in the presence of MG132 (Fig. 4B). Next, to investigate whether UCP3 is indeed ubiquitinated *in vivo*, ubiquitination assays based on co-immunoprecipitated UCP3 were carried out with the skeletal muscles from the three groups of mice. As presented in Fig. 4C, HFD efficiently ubiquitinated UCP3, supporting that high-fat-intake did deteriorate UCP3 protein stability by accelerating degradation; especially, insulin was observed to greatly attenuate HFD-induced UCP3 ubiquitination, implying the potential involvement of the ubiquitin-proteasome pathway in the recovery of UCP3 protein by insulin.

Furthermore, to determine the role of UCP3 in the restoration of AMPK phosphorylation by insulin, its expression was knocked down with siRNA in L6 myotubes. Insulin-induced stimulation of AMPK phosphorylation was profoundly impeded in the absence of UCP3 (Fig. 4D). These data suggested that the increased UCP3 protein expression was responsible for the repression of mitochondrial membrane potential and it mediated the recovered phosphorylation of AMPK elicited by insulin.

Altogether, insulin protected UCP3 from ubiquitination degradation, thereby uncoupling mitochondrial oxidative phosphorylation with a decline in cellular ATP. Sequentially, increased AMPK phosphorylation underlies the promising effect of early insulin therapy on lipid homeostasis in skeletal muscle (Fig. 5).

Discussion

In contrast to the conventional perspective that insulin promotes lipid deposition physiologically, a plethora of clinical data and animal models imply that early insulin administration improves the lipid profile and reduces lipid content in metabolically active tissues of diabetic subjects (4,30,37). However, the molecular mechanism of insulin action is not yet fully understood. The present study provided mechanistic insight into the protective action of insulin in sustaining muscular lipid homeostasis, which was in correlation with abating energy surplus evoked by fatty acid overload, followed by AMPK-mediated augmentation of fatty acid oxidation and attenuation of lipogenesis. The recovery of UCP3 expression was found to be responsible for the decline in the cellular energy charge of insulin. This suggests an active role of insulin in improving lipotoxicity of skeletal muscle, especially in the early development of insulin resistance.

Mitochondria have received increased attention in order to understand the etiology of obesity-associated insulin resistance owing to its central role in lipid utilization and energy production. Several pieces of evidence have linked a compromised mitochondrial function to the development of insulin resistance (38,39), which is recognized as a dynamic alteration of mitochondrial function adapted to oscillations in energy demand and substrate availability, termed as mitochondrial plasticity (39). The initial stage of HFD-induced obesity is continually associated with mitochondrial over-activation and concomitant energy surplus (40). Consistently, we observed a high energy charge and ATP content, which was generated from stimulating activities of complex III and IV and coupling process in skeletal muscle cells treated with excessive fatty acid *in vivo* and *in vitro*; increased ATP inhibits the phosphorylation of AMPK. The anabolic pathways are driven by utilizing ATP to store glycogen and lipid as energy sources

and balance the energy supply with demand. Nevertheless, this is detrimental to insulin sensitivity with prolonged duration. Thus, blocking excessive ATP synthesis provides a latent approach to alleviate insulin resistance.

Multiple anti-diabetic agents, involving metformin and resveratrol, have been demonstrated to improve insulin sensitivity via declining cellular energy state. The underlying mechanisms by which metformin and berberine diminish glyconeogenesis in the liver and triglyceride accumulation in skeletal muscle was found to include interruption of the activity of mitochondrial complex I, resulting in decreased ATP production (41-45). Resveratrol was documented to block ATP synthase activity, thereby inhibiting mitochondrial ATP synthesis (46). Nevertheless, the conclusions concerning the effect of insulin on mitochondrial oxidative phosphorylation are yet controversial. During hyperinsulinemic-euglycemic clamp, insulin was found to promote ATP production, accompanied by upregulated complex IV activity in skeletal muscles of healthy subjects (29) while patients with overt T2DM and their first-degree relatives failed to show an increased mitochondrial activity (28,47). Conversely, intensive insulin therapy for 10 days increased muscular mRNA levels of complex I, III and V in diabetics (48). Taken together, the impact of insulin on mitochondria, at least partially, depends on the concentration, method, and duration of administration. Moreover, the duration of T2DM at the time of intervention may also influence the impact of insulin on energy metabolism owing to long-term glycemic remission in patients with newly diagnosed rather than prolonged T2DM, induced by insulin therapy (49). In our rodent model of early-stage diabetes, insulin mitigated the muscular energy surplus, subsequently, improving AMPK signaling. However, whether this action of insulin persists in the later event of diabetes needs to be clarified in the future. Additionally, the convergence of insulin and metformin, both targeting a decreased energy state, may potentially provide a synergistic therapeutic effect on insulin resistance, which still necessitates further evaluation.

Different from metformin or resveratrol, our study indicated that the protective role of early insulin intervention in muscular bioenergy was disassociated from the expression or activities of respiratory complexes. On the other hand, insulin, by restoring UCP3 protein expression, enhanced the cellular uncoupling process in rodent myocytes provided with abundant fatty acid. Mitochondrial uncoupling serves to reduce the efficiency of ATP synthesis by decreasing the proton motive force. Likewise, in this study, the elevation of mitochondrial membrane potential in insulin-resistant skeletal muscle cells was annulled after insulin administration, despite the lack of comprehensive evaluation for systematic energy expenditure and respiratory control. Currently, uncoupling has become an appealing therapeutic target to facilitate energy turnover, improving insulin sensitivity as a consequence. Hence, exploring chemical mitochondrial uncouplers and evaluating their potential clinical application are critical for T2DM prevention and treatment. Dinitrophenol, a non-selective mitochondrial uncoupler, effectively boosts the energy expenditure without generating ATP and was approved for treating obesity in the 1930s (50). However, at high dosages, dinitrophenol causes hyperthermia that precludes its therapeutic usage. Until recently, one study reported that a liver-targeted derivative of dinitrophenol alleviated fatty liver and whole-body insulin resistance in HFD rats with a wide therapeutic index, thereby providing a basis for exploiting tissue-targeted mitochondrial uncoupling agents (51). Alternatively, oral niclosamide ethanolamine, derived from niclosamide which uncouples mitochondria of parasitic worms and serves as an anthelmintic drug, was observed to improve the hepatic steatosis and glycemic control with little impact on body temperature in insulin-resistant mice (52). Moreover, curcumin has been shown to uncouple the oxidative phosphorylation at low concentrations in isolated rat liver mitochondria (53,54). The resulting increase in the AMP:ATP ratio could explain its activation in AMPK signaling. Notwithstanding these encouraging results in animal models, the hypothesis that chemical uncouplers may contribute to improved insulin sensitivity and their safety in clinical practice necessitate further substantiation by experimental data in humans.

In conclusion, UCP3-induced energy collapse, accompanied by a relief in AMPK inhibition, was found to be associated with the positive effect of insulin on muscular lipotoxicity. This study suggests that obstruction of an energy surplus is involved in the benefits of early insulin therapy on lipid regulation, which supports the idea that energy homeostasis could be a therapeutic target for obesity and T2DM.

Acknowledgements

This study was supported by grants from the National Natural Science Foundation of China (nos. 81570736, 81570737, 81370947, 81270906, 81600632, 81600637, 81500612 and 81400832), the National Key Research and Development Program of China (no. 2016YFC1304804), the Project of National Key Clinical Division, Jiangsu Province's Key Discipline of Medicine (no. XK201105), China Diabetes Young Scientific Talent Research Project, the Key Research and Development Program of Jiangsu Province of China (nos. BE2015604 and BE2016606), the Key Provincial Talents Program of Jiangsu Province of China (no. RC2011011), the Jiangsu Province's Key Laboratory for Molecular Medicine (no. BM2007208), the Nanjing Science and Technology Development Project (no. 201605019) and the Key Project of Nanjing Clinical Medical Science.

References

1. Guariguata L, Whiting DR, Hambleton I, Beagley J, Linnenkamp U and Shaw JE: Global estimates of diabetes prevalence for 2013 and projections for 2035. Diabetes Res Clin Pract 103: 137-149, 2014.
2. Kramer CK, Zinman B and Retnakaran R: Short-term intensive insulin therapy in type 2 diabetes mellitus: A systematic review and meta-analysis. Lancet Diabetes Endocrinol 1: 28-34, 2013.
3. Hu Y, Li L, Xu Y, Yu T, Tong G, Huang H, Bi Y, Weng J and Zhu D: Short-term intensive therapy in newly diagnosed type 2 diabetes partially restores both insulin sensitivity and β-cell function in subjects with long-term remission. Diabetes Care 34: 1848-1853, 2011.
4. Weng J, Li Y, Xu W, Shi L, Zhang Q, Zhu D, Hu Y, Zhou Z, Yan X, Tian H, *et al*: Effect of intensive insulin therapy on beta-cell function and glycaemic control in patients with newly diagnosed type 2 diabetes: A multicentre randomised parallel-group trial. Lancet 371: 1753-1760, 2008.
5. Samuel VT, Petersen KF and Shulman GI: Lipid-induced insulin resistance: Unravelling the mechanism. Lancet 375: 2267-2277, 2010.

6. Shulman GI, Rothman DL, Jue T, Stein P, DeFronzo RA and Shulman RG: Quantitation of muscle glycogen synthesis in normal subjects and subjects with non-insulin-dependent diabetes by 13C nuclear magnetic resonance spectroscopy. N Engl J Med 322: 223-228, 1990.
7. Eckardt K, Taube A and Eckel J: Obesity-associated insulin resistance in skeletal muscle: Role of lipid accumulation and physical inactivity. Rev Endocr Metab Disord 12: 163-172, 2011.
8. Itani SI, Ruderman NB, Schmieder F and Boden G: Lipid-induced insulin resistance in human muscle is associated with changes in diacylglycerol, protein kinase C, and IkappaB-alpha. Diabetes 51: 2005-2011, 2002.
9. Samuel VT and Shulman GI: Mechanisms for insulin resistance: Common threads and missing links. Cell 148: 852-871, 2012.
10. Guillet-Deniau I, Mieulet V, Le Lay S, Achouri Y, Carré D, Girard J, Foufelle F and Ferré P: Sterol regulatory element binding protein-1c expression and action in rat muscles: Insulin-like effects on the control of glycolytic and lipogenic enzymes and UCP3 gene expression. Diabetes 51: 1722-1728, 2002.
11. Guillet-Deniau I, Pichard AL, Koné A, Esnous C, Nieruchalski M, Girard J and Prip-Buus C: Glucose induces de novo lipogenesis in rat muscle satellite cells through a sterol-regulatory-element-binding-protein-1c-dependent pathway. J Cell Sci 117: 1937-1944, 2004.
12. Tsintzas K, Jewell K, Kamran M, Laithwaite D, Boonsong T, Littlewood J, Macdonald I and Bennett A: Differential regulation of metabolic genes in skeletal muscle during starvation and refeeding in humans. J Physiol 575: 291-303, 2006.
13. Bruce CR, Anderson MJ, Carey AL, Newman DG, Bonen A, Kriketos AD, Cooney GJ and Hawley JA: Muscle oxidative capacity is a better predictor of insulin sensitivity than lipid status. J Clin Endocrinol Metab 88: 5444-5451, 2003.
14. Kim JY, Hickner RC, Cortright RL, Dohm GL and Houmard JA: Lipid oxidation is reduced in obese human skeletal muscle. Am J Physiol Endocrinol Metab 279: E1039-E1044, 2000.
15. Ukropcova B, Sereda O, de Jonge L, Bogacka I, Nguyen T, Xie H, Bray GA and Smith SR: Family history of diabetes links impaired substrate switching and reduced mitochondrial content in skeletal muscle. Diabetes 56: 720-727, 2007.
16. Li Y, Xu S, Mihaylova MM, Zheng B, Hou X, Jiang B, Park O, Luo Z, Lefai E, Shyy JY, *et al*: AMPK phosphorylates and inhibits SREBP activity to attenuate hepatic steatosis and atherosclerosis in diet-induced insulin-resistant mice. Cell Metab 13: 376-388, 2011.
17. Ronnett GV, Kleman AM, Kim EK, Landree LE and Tu Y: Fatty acid metabolism, the central nervous system, and feeding. Obesity (Silver Spring) 14 (Suppl 5): 201S-207S, 2006.
18. Kjøbsted R, Pedersen AJ, Hingst JR, Sabaratnam R, Birk JB, Kristensen JM, Højlund K and Wojtaszewski JF: Intact regulation of the AMPK signaling network in response to exercise and insulin in skeletal muscle of male patients with type 2 diabetes: Illumination of AMPK activation in recovery from exercise. Diabetes 65: 1219-1230, 2016.
19. Tang S, Wu W, Tang W, Ge Z, Wang H, Hong T, Zhu D and Bi Y: Suppression of Rho-kinase 1 is responsible for insulin regulation of the AMPK/SREBP-1c pathway in skeletal muscle cells exposed to palmitate. Acta Diabetol: Mar 7, 2017 (Epub ahead of print).
20. Saltiel AR: New therapeutic approaches for the treatment of obesity. Sci Transl Med 8: 323rv2, 2016.
21. Busiello RA, Savarese S and Lombardi A: Mitochondrial uncoupling proteins and energy metabolism. Front Physiol 6: 36, 2015.
22. Krook A, Digby J, O'Rahilly S, Zierath JR and Wallberg-Henriksson H: Uncoupling protein 3 is reduced in skeletal muscle of NIDDM patients. Diabetes 47: 1528-1531, 1998.
23. Mensink M, Hesselink MK, Borghouts LB, Keizer H, Moonen-Kornips E, Schaart G, Blaak EE and Schrauwen P: Skeletal muscle uncoupling protein-3 restores upon intervention in the prediabetic and diabetic state: Implications for diabetes pathogenesis? Diabetes Obes Metab 9: 594-596, 2007.
24. Schrauwen P, Hesselink MK, Blaak EE, Borghouts LB, Schaart G, Saris WH and Keizer HA: Uncoupling protein 3 content is decreased in skeletal muscle of patients with type 2 diabetes. Diabetes 50: 2870-2873, 2001.
25. Clapham JC, Arch JR, Chapman H, Haynes A, Lister C, Moore GB, Piercy V, Carter SA, Lehner I, Smith SA, *et al*: Mice overexpressing human uncoupling protein-3 in skeletal muscle are hyperphagic and lean. Nature 406: 415-418, 2000.
26. Costford SR, Chaudhry SN, Salkhordeh M and Harper ME: Effects of the presence, absence, and overexpression of uncoupling protein-3 on adiposity and fuel metabolism in congenic mice. Am J Physiol Endocrinol Metab 290: E1304-E1312, 2006.
27. Son C, Hosoda K, Ishihara K, Bevilacqua L, Masuzaki H, Fushiki T, Harper ME and Nakao K: Reduction of diet-induced obesity in transgenic mice overexpressing uncoupling protein 3 in skeletal muscle. Diabetologia 47: 47-54, 2004.
28. Petersen KF, Dufour S and Shulman GI: Decreased insulin-stimulated ATP synthesis and phosphate transport in muscle of insulin-resistant offspring of type 2 diabetic parents. PLoS Med 2: e233, 2005.
29. Stump CS, Short KR, Bigelow ML, Schimke JM and Nair KS: Effect of insulin on human skeletal muscle mitochondrial ATP production, protein synthesis, and mRNA transcripts. Proc Natl Acad Sci USA 100: 7996-8001, 2003.
30. Bi Y, Cai M, Liang H, Sun W, Li X, Wang C, Zhu Y, Chen X, Li M and Weng J: Increased carnitine palmitoyl transferase 1 expression and decreased sterol regulatory element-binding protein 1c expression are associated with reduced intramuscular triglyceride accumulation after insulin therapy in high-fat-diet and streptozotocin-induced diabetic rats. Metabolism 58: 779-786, 2009.
31. Bi Y, Wu W, Shi J, Liang H, Yin W, Chen Y, Tang S, Cao S, Cai M, Shen S, *et al*: Role for sterol regulatory element binding protein-1c activation in mediating skeletal muscle insulin resistance via repression of rat insulin receptor substrate-1 transcription. Diabetologia 57: 592-602, 2014.
32. Xie B, Chen Q, Chen L, Sheng Y, Wang HY and Chen S: The Inactivation of RabGAP function of AS160 promotes lysosomal degradation of GLUT4 and causes postprandial hyperglycemia and hyperinsulinemia. Diabetes 65: 3327-3340, 2016.
33. Livak KJ and Schmittgen TD: Analysis of relative gene expression data using real-time quantitative PCR and the 2(-Delta Delta C(T)) method. Methods 25: 402-408, 2001.
34. Bhatt DP, Chen X, Geiger JD and Rosenberger TA: A sensitive HPLC-based method to quantify adenine nucleotides in primary astrocyte cell cultures. J Chromatogr B Analyt Technol Biomed Life Sci 889-890: 110-115, 2012.
35. Azzu V, Mookerjee SA and Brand MD: Rapid turnover of mitochondrial uncoupling protein 3. Biochem J 426: 13-17, 2010.
36. Mookerjee SA and Brand MD: Characteristics of the turnover of uncoupling protein 3 by the ubiquitin proteasome system in isolated mitochondria. Biochim Biophys Acta 1807: 1474-1481, 2011.
37. Bi Y, Sun WP, Chen X, Li M, Liang H, Cai MY, Zhu YH, He XY, Xu F and Weng JP: Effect of early insulin therapy on nuclear factor kappaB and cytokine gene expressions in the liver and skeletal muscle of high-fat diet, streptozotocin-treated diabetic rats. Acta Diabetol 45: 167-178, 2008.
38. Pagel-Langenickel I, Bao J, Pang L and Sack MN: The role of mitochondria in the pathophysiology of skeletal muscle insulin resistance. Endocr Rev 31: 25-51, 2010.
39. Szendroedi J, Phielix E and Roden M: The role of mitochondria in insulin resistance and type 2 diabetes mellitus. Nat Rev Endocrinol 8: 92-103, 2011.
40. Zhang Y and Ye J: Mitochondrial inhibitor as a new class of insulin sensitizer. Acta Pharm Sin B 2: 341-349, 2012.
41. Bridges HR, Jones AJ, Pollak MN and Hirst J: Effects of metformin and other biguanides on oxidative phosphorylation in mitochondria. Biochem J 462: 475-487, 2014.
42. Foretz M, Hébrard S, Leclerc J, Zarrinpashneh E, Soty M, Mithieux G, Sakamoto K, Andreelli F and Viollet B: Metformin inhibits hepatic gluconeogenesis in mice independently of the LKB1/AMPK pathway via a decrease in hepatic energy state. J Clin Invest 120: 2355-2369, 2010.
43. Owen MR, Doran E and Halestrap AP: Evidence that metformin exerts its anti-diabetic effects through inhibition of complex 1 of the mitochondrial respiratory chain. Biochem J 348: 607-614, 2000.
44. Turner N, Li JY, Gosby A, To SW, Cheng Z, Miyoshi H, Taketo MM, Cooney GJ, Kraegen EW, James DE, *et al*: Berberine and its more biologically available derivative, dihydroberberine, inhibit mitochondrial respiratory complex I: A mechanism for the action of berberine to activate AMP-activated protein kinase and improve insulin action. Diabetes 57: 1414-1418, 2008.
45. Xia X, Yan J, Shen Y, Tang K, Yin J, Zhang Y, Yang D, Liang H, Ye J and Weng J: Berberine improves glucose metabolism in diabetic rats by inhibition of hepatic gluconeogenesis. PLoS One 6: e16556, 2011.

46. Gledhill JR, Montgomery MG, Leslie AG and Walker JE: Mechanism of inhibition of bovine F1-ATPase by resveratrol and related polyphenols. Proc Natl Acad Sci USA 104: 13632-13637, 2007.
47. Szendroedi J, Schmid AI, Chmelik M, Toth C, Brehm A, Krssak M, Nowotny P, Wolzt M, Waldhausl W and Roden M: Muscle mitochondrial ATP synthesis and glucose transport/phosphorylation in type 2 diabetes. PLoS Med 4: e154, 2007.
48. Sreekumar R, Halvatsiotis P, Schimke JC and Nair KS: Gene expression profile in skeletal muscle of type 2 diabetes and the effect of insulin treatment. Diabetes 51: 1913-1920, 2002.
49. Retnakaran R and Zinman B: Short-term intensified insulin treatment in type 2 diabetes: Long-term effects on β-cell function. Diabetes Obes Metab 14 (Suppl 3): 161-166, 2012.
50. Parascandola J: Dinitrophenol and bioenergetics: An historical perspective. Mol Cell Biochem 5: 69-77, 1974.
51. Perry RJ, Kim T, Zhang XM, Lee HY, Pesta D, Popov VB, Zhang D, Rahimi Y, Jurczak MJ, Cline GW, *et al*: Reversal of hypertriglyceridemia, fatty liver disease, and insulin resistance by a liver-targeted mitochondrial uncoupler. Cell Metab 18: 740-748, 2013.
52. Tao H, Zhang Y, Zeng X, Shulman GI and Jin S: Niclosamide ethanolamine-induced mild mitochondrial uncoupling improves diabetic symptoms in mice. Nat Med 20: 1263-1269, 2014.
53. Ligeret H, Barthélémy S, Bouchard Doulakas G, Carrupt PA, Tillement JP, Labidalle S and Morin D: Fluoride curcumin derivatives: New mitochondrial uncoupling agents. FEBS Lett 569: 37-42, 2004.
54. Lim HW, Lim HY and Wong KP: Uncoupling of oxidative phosphorylation by curcumin: Implication of its cellular mechanism of action. Biochem Biophys Res Commun 389: 187-192, 2009.